Natural Dyes as Photosensitizers for Dye-sensitized Solar Cells

Hatem S. El-Ghamri[1,2], Sofyan A. Taya[1,2,*], Taher M. El-Agez[1,2], Amal M. Al-Kahlout[3],
Naji Al Dahoudi[3], Monzir S. Abdel-Latif[2,4]

[1] *Physics Department, Islamic University of Gaza, Gaza, Palestinian Authority*
[2] *Renewable Energy Center, Islamic University of Gaza, Gaza, Palestinian Authority*
[3] *Physics Department, Al Azhar University, Gaza, Palestinian Authority*
[4] *Chemistry Department, Islamic University of Gaza, Gaza, Palestinian Authority*

Dye-sensitized solar cells (DSSCs) were assembled using Zinc oxide (ZnO) nanoparticles as a photoelectrode and natural dyes extracted from eight natural plants as photosensitizers. The structural properties of the synthesized ZnO nanoparticles were studied using XRD, SEM and TEM characterizations. Photovoltaic parameters such as short circuit current density J_{sc}, open circuit voltage V_{oc}, fill factor *FF*, and overall conversion efficiency η for the fabricated cells were determined under 100 mW/cm² illumination. It was found that the DSSC fabricated with the extracted safflower dye as a sensitizer showed the best performance. Also, its performance increased with increasing the sintering temperature of the semiconductor electrode with highest performance at 400 °C. Moreover, it was found that a semiconductor electrode of 7.5 μm thickness yielded the highest response.

Keywords: Dye-sensitized solar cell, Natural dye, ZnO.

PACS number: 84.60.Jt

1. INTRODUCTION

A solar cell is a device that converts sunlight into electricity. Materials used in photovoltaic devices are mainly semiconductors including, among others, crystalline silicon, III-V compounds, copper indium selenide / sulfide, and cadmium telluride [1-3]. Low-cost solar cells have been the subject of intensive research work for the last decades. Amorphous semiconductors were announced to be one of the most promising materials for low-cost energy production. Recently dye sensitized solar cells (DSSCs) emerged as a new type of low cost solar cells with simple preparation procedures. The DSSC operation is based on the sensitization of wide bandgap semiconductors such as TiO₂ or ZnO [4]. The performance of the cell is mainly dependent on the dye used as sensitizer in addition to many parameters, like the photoelectrode materials, the redox and the backelectrode. The absorption spectrum of the dye and its anchorage to the surface of TiO₂ or ZnO are the most important parameters determining the efficiency of the DSSC [5].

Generally, transition metal coordination compounds such as ruthenium polypyridyl complexes are used as sensitizers, due to their highly efficient metal-to-ligand charge transfer and intense charge-transfer absorption in the whole visible range [6]. However, ruthenium polypyridyl complexes contain a heavy metal, which is undesirable for environmental aspects [7]. Moreover, the synthesizing process of these complexes is complicated and expensive. Alternatively, natural dyes may be used for the same purpose with an acceptable efficiency [5-17]. The advantages of natural dyes include their low cost and availability [6]. The sensitization of wide bandgap semiconductors using natural pigments is usually ascribed to anthocyanins which belong to the group of natural dyes responsible for several colors in the red-blue range, found in flowers, leaves, and fruits [5-19]. Hydroxyl and carbonyl groups present in the anthocyanin molecule can bind to the surface of a porous TiO₂ or ZnO film. This facilitates electron transfer from the anthocyanin molecule to the conduction band of the semiconductor [6]. Anthocyanins from various plants gave different sensitization performances. However, there is no acceptable explanation behind such results, so far [18].

In this work, DSSCs were prepared using different natural dyes extracted from plants. ZnO layers were sensitized using eight natural dyes. The absorption spectra of these dyes were obtained. The *J-V* characteristic curves were measured and the corresponding output power was determined. The efficiency of each DSSC corresponding to each dye is calculated. Then, the effect of the sintering temperature of the photoelectrode and its thickness were investigated using DSSCs sensitized with safflower.

2. EXPERIMENTAL

2.1 Extraction of Natural Dye Sensitizers

The natural dyes used in this study were extracted from the following plants: Safflower (Cathumus tincrorius), Senna (Cassia angustifolia), Calumus draca (Dracaena oinnabari), Carya illinoensis, Rheum, Roselle (Hibiscas sabdarriffa), Rosa damascena, and Runica granatum. The raw natural materials were first washed with distilled water and then dried at 70 °C. After crushing into fine powder in a mortar, 1 gm from each material was immersed in 5 ml of ethyl alcohol at room temperature and in dark for one day. After filtration of the solutions, natural dyes were obtained [6, 8, 19]. Dye solutions were protected from direct light exposure.

* staya@iugaza.edu.ps

2.2 Synthesis and Characterization of ZnO Nanoparticles

ZnO nanoparticles used in this article have been synthesized at pH 12 following the procedure described by Rani et al. [20] by dissolving 4.4 g of zinc acetate dihydrate, reagent $Zn(CH_3COO)_{2.2}H_2O$ (ACROS) in 100 mL of methanol to obtain a 0.22 M sol which was stirred overnight. Details of the preparation procedure can be found elsewhere [20-22]. A mortar was used to grind the powder to reduce the size of the agglomerates in order to get a fine powder.

X-ray diffraction (XRD) patterns of the powder were collected by means of a Bruker AXS D8 powder diffractometer unit, using Cu Kα radiation ($\lambda = 0.154$ nm), operating at 40 kV and 40 mA. A position sensitive detector (LynxEye) based on Bruker AXS compound silicon strip technology was used. The ZnO powders supported on glass holders were scanned between $2\theta = 10°$ to 100° with a 2θ scan step size of 0.005°. The structural refinement of the obtained phases and profile analysis of the related diffraction patterns were carried out using the program TOPAS, and the mean crystallite sizes were calculated using the Scherrer equation (Scherrer constant $k = 1$).

The surface morphology and the size of ZnO particles were analyzed using a high resolution scanning electron microscopy HR-SEM (JSM67500F, JEOL) using secondary electron signal excited by a 10 keV primary beam, at operating potential of 15 kV. The morphology of the particles and the particle size were determined using transmission electron microscopy TEM (HRTEM-CM200 FEG, Philips) operating at 200 kV.

2.3 Preparation of Dye Sensitized Solar Cells

FTO conductive glass sheets were cut into pieces of dimensions 0.8 cm × 1.6 cm. The samples were cleaned in a detergent solution using an ultrasonic bath for 15 min, rinsed with water and ethanol, and then dried. The ZnO paste was prepared by adding 0.062 g of ZnO nano-powder and 0.072 g of polyethylene glycol then grinding the mixture for half an hour until a homogeneous paste was obtained. Thin layers of the prepared ZnO past were spread on the transparent conducting FTO coated glass by employing doctor blade method. Samples were then dried in an oven at 70 °C for 20 min. Finally, the samples were sintered at 400 °C for 40 min then were cooled down to 70 °C before being placed in dye solutions for one day under dark. The dyed ZnO electrode and a sputtered platinum counter electrode were assembled to form a solar cell by sandwiching a redox (I^- / I^3) electrolyte solution. The electrolyte solution is composed of 2 ml acetonitrile (ACN), 8 ml propylene carbonate (*p*-carbonate), 0.668 gm (LiI), and 0.0634 gm (I_2).

2.4 Characterization and Measurement

The UV-VIS absorption spectra of the eight dyes were measured using a UV-VIS spectrophotometer (Thermoline Genesys 6). The wavelength range of absorption spectra analysis extends from 350-800 nm. The *I-V* characteristic curves under illumination were conducted using National Instruments data acquisition card (USB NI 6251) in combination of a Labview program. The *I-V* curves were measured at 100 mW/cm² irradiations using high pressure mercury arc lamp. The fill factor (*FF*) defined as

$$FF = \frac{I_{mp}.V_{mp}}{I_{sc}.V_{oc}}, \tag{1}$$

is calculated from the *I-V* curve of each cell, where I_{mp} and V_{mp} are the photocurrent and photovoltage at the maximum power output and I_{sc} and V_{oc} are the short circuit photocurrent and open circuit photovoltage, respectively. The energy conversion efficiency (η) is defined as follows

$$\eta = \frac{FF.I_{sc}.V_{oc}}{P_{in}}, \tag{2}$$

where P_{in} is the power of incident light.

3. RESULTS AND DISCUSSIONS

3.1 Absorption Spectra of Natural Dyes

The UV-VIS absorption spectra of the extracts of Safflower (Cathumus tincrorius), Senna (Cassia angustifolia), Roselle (Hibiscas sabdarriffa), Rheum, Calumus draca (Dracaena oinnabari), Rosa damascena, Carya illinoensis, and Runica granatum dissolved in ethyl alcohol as solvent are shown in Fig. 1. It can be seen from the figure that the absorption peak for the extract of Safflower is located at about 428.8 nm. The absorption spectrum of Senna showed a shoulder at 410.8 nm and a peak at 664.7 nm. The extract of Roselle showed a peak at 512.6 nm. The extract of Rheum shows an absorption peak at 422.2 nm. It is obvious that the extract of Calumus draca exhibits an absorption peak at 492 nm. Also, no pronounced peaks are shown for extracts of Rosa damascene, Carya illinoensis, and Runica granatum.

When ZnO photoelectrode was dyed with Safflower, the absorption spectrum was carried out again for the photoelectrode layer. Fig. 2 shows a comparison between U-VIS spectrum of Safflower in ethyl alcohol and the UV-VIS spectrum of the ZnO film dyed with safflower. It is clear that the spectrum of the dyed film has a peak at 408 nm shifted from the spectra of the dye solution. The observed hyperchromic shift is typical for adsorbed dyes on solid substrates.

3.2 ZnO Powder Structure

Figure 3 illustrates the XRD pattern of the synthesized ZnO nanopowder. The figure reveals that the powder is highly crystalline and that its structure is in accordance with the typical wurtzite hexagonal structure (JCPDS No. 0036– 1451 WL 15406 Hexagonal-03 24982). The crystallite mean value is found to be 12 nm and the crystallite size calculated for the (101) and (002) peaks are found to be 12 nm and 11 nm, respectively. The lattice dimensions are found to be [$a = b = 3.253(0)$ Å, and $c = 5.213(4)$ Å].
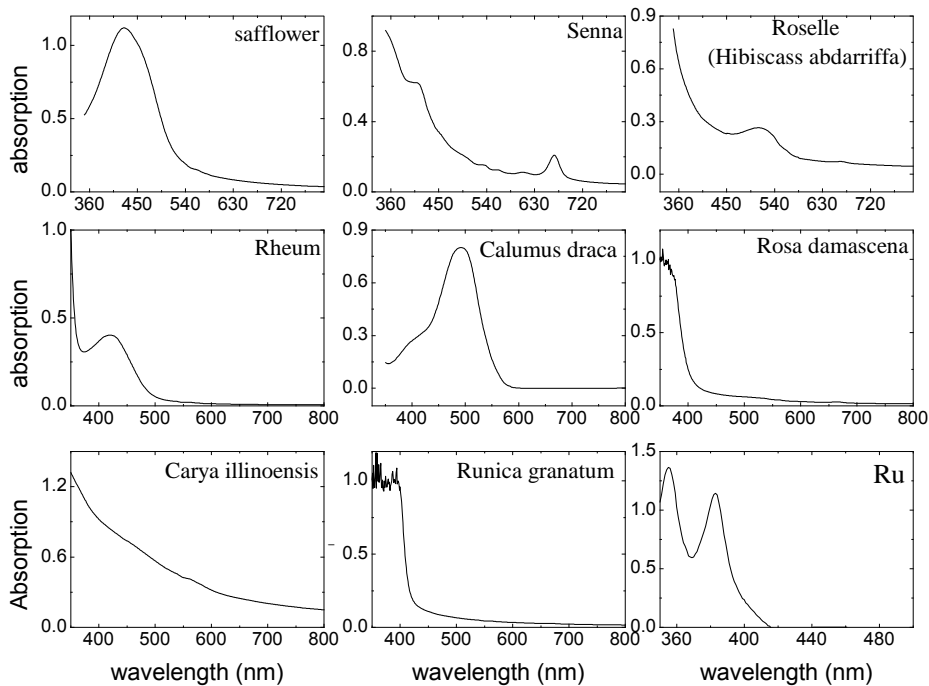
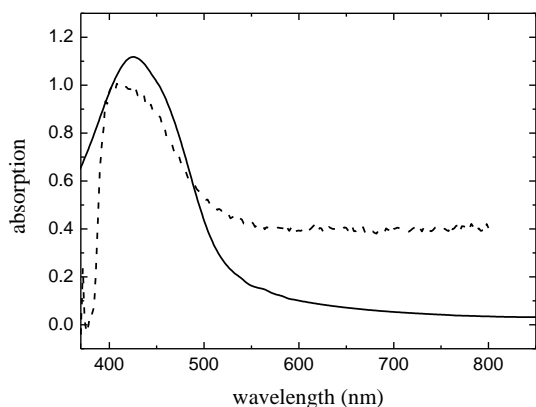**Fig. 1** – UV-VIS absorption spectra of all dyes in ethyl alcohol solution

Fig. 2 – The absorption spectrum of safflower in ethyl alcohol (solid line) and safflower adsorbed on ZnO layer (dashed line)
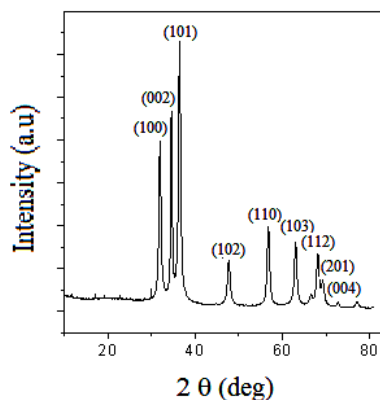

Fig. 3 – XRD pattern of ZnO powder synthesized at room temperature and pH 12, then dried at 100 °C in air. The peaks corresponds to the hexagonal- wurtzite structure in the reference data (JCPDS No.0036–1451)

3.3 Surface Morphology and BET Surface Area Analyses of ZnO Powder

It is very important to investigate the Surface morphology and Brunauer-Emmelt-Teller (BET) surface area of the ZnO powder since they are considered the key points for DSSC application. The BET surface area of the ZnO powder prepared at pH 12 and dried at 100 °C was 42.3 m² g⁻¹. This value is higher than the 23.8 m² g⁻¹ reported by Agha Baba Zadeh et al. [23] for powders obtained by mechanochemical processing and sintered at 400 °C. This difference can be due to agglomeration of nanoparticles during sintering process which accordingly reduce the surface area. A SEM picture for the ZnO powder is shown in Fig. 4. As can be seen from the figure the nanoparticles are homogeneous and well defined with size of about 15 nm. Figure 5 illustrates the TEM micrograph of the powder. The figure shows that the powder has a porous agglomerate structure consisting mainly of spherical crystalline particles with about 15-20 nm diameter.
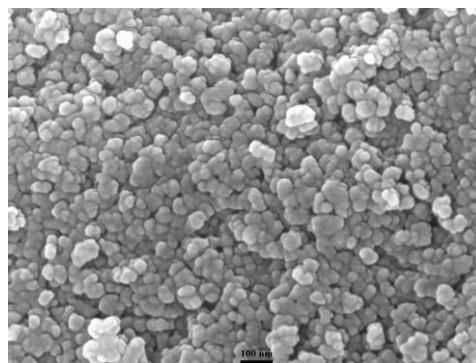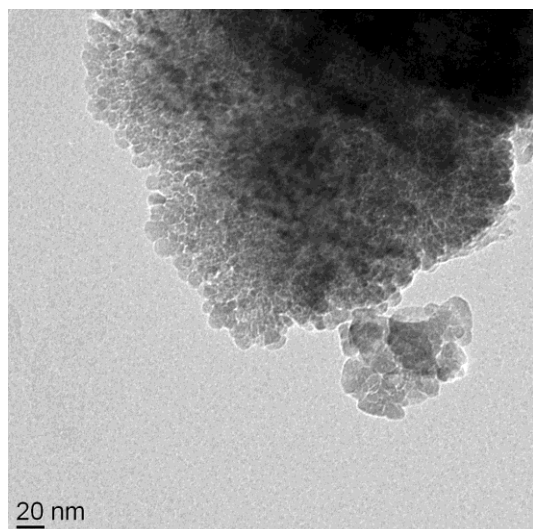

Fig. 4 – SEM images of the nanostructured ZnO powder synthesized at pH 12. The scale bars correspond to 100 nm

Fig. 5 – TEM image of the nanostructured ZnO powder synthesized at pH 12 and dried at 100 °C for 12 h. The scale bar corresponds to 20 nm

3.4 Photovoltaic Properties

The performance of the natural sensitizers in the photoelectrochemical solar cells was monitored through electrical current and voltage outputs under 100 mW/cm² illuminations. Figures 6 and 7 show the current density-voltage (*J-V*) characteristic curves of the assembled DSSCs sensitized with natural dye extracts. It is clear from these figures that the DSSC sensitized with safflower extracts exhibit the highest *J-V* response. Table 1 presents all the photoelectrochemical parameters of the fabricated DSSCs assembled by photoanodes with ZnO sensitized by the natural dyes extracted with ethyl alcohol. These parameters are the photocurrent density, J_{sc}, open circuit voltage, V_{oc}, fill-factor (*FF*), and the cell efficiency (η). It is shown in Table 1, that the DSSC sensitized with safflower shows the highest photoelectrochemical performance among the DSSCs ($J_{sc} = 1$ mA/cm², $V_{oc} = 0.390$ V, $FF = 0.24$, and $\eta = 0.1$). It should be pointed out that Safflower (Cathumus tincrorius) has the molecular Formula $C_{43}H_{42}O_{22}$. It's a member of the family of Compositae or Asteraceae. Safflower was the Latinized synonym of the Arabic word quartum, or gurtum, which refers to the color of the dye extracted from safflower flowers. The English name safflower probably evolved from various written forms of usfar, affore, asfiore, and saffiore to safflower. Safflower flowers are known to have many medical properties for curing several chronic diseases and they are widely used in Chinese herbal preparations. Safflower oil is characterized by the presence of a high proportion of n-6 polyunsaturated fatty acids that include linoleic (approximately 75 %), oleic (13 %), palmitic (6 %), stearic (3 %), and other minor straight-chained fatty acids [24]. Alpha and gamma tocopherol content have also been found [25].

It is noted that the natural dye of Roselle (Hibiscassabdarriffa) extracted by polyethylene glycol interacts with the zinc oxide layer, causing corrosion of this layer.
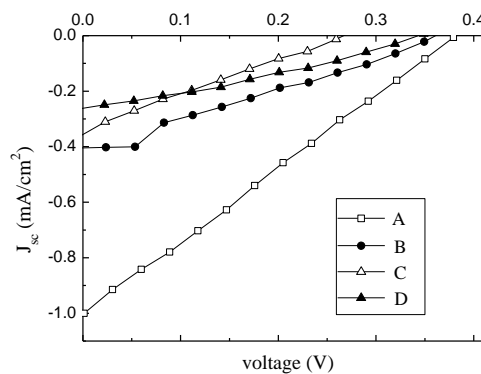
Fig. 6 – Current density-voltage curves for the DSSCs sensitized by four natural extracts: (A) safflower, (B) Senna, (C) Rheum and (D) Calumusdraca at intensity of the incident light of 100 mW cm⁻². Natural extracts were prepared using ethyl alcohol
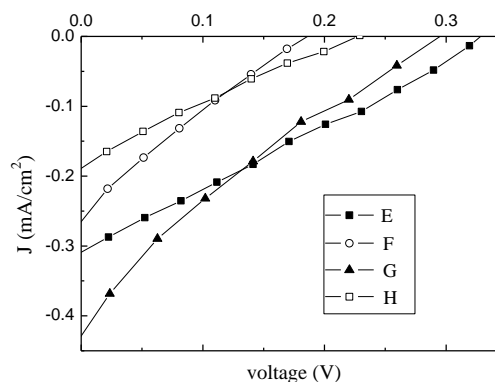
Fig. 7 – Current density-voltage curves for the DSSCs sensitized by four natural extracts (E) Calumus draca, (F) Rosa damascena, (G) Carya illinoensis, (H) Runica granatum at intensity of the incident light of 100 mW cm⁻². Natural extracts were prepared using ethyl alcohol

3.5 Photoelectrode Sintering Temperature and Thickness Effects on the Performance of the Safflower Sensitized DSSC

A. Effect of the Sintering Temperature

ZnO nanoparticles paste was prepared by dispersing ZnO nanoparticles in polyethylene glycol at 1 : 1 ratio by weight. Then, each photoelectrode was sintered at different temperatures (250, 300, 350, 400, 450, 500, and 600 °C) for about 30 min in each case. The sintering process was followed by dying the sample in safflower extract which exhibited the best performance among the other extracts. Figure 8 illustrates the photoelectrical response at 100 mW/cm² for different sintering temperatures. It is clear that the highest response is obtained for the DSSC with photoelectrode sintered at 400 °C. This sintering temperature may attain the largest surface area and highest porosity, which is required for more dye loading to get higher photocurrent density. Further increasing the sintering temperature decreases the cell efficiency, which is a result of the reduction of the surface area, because more particles are getting in contact and therefore losing the infiltration of the dye inside the pores. Values of current densities and open circuit voltages are shown at various sintering temperature values in Table 2.

Table 1 – Photoelectrochemical parameters of the DSSCs sensitized by natural dyes extracted with ethyl alcohol as solvent

Natural dye	J_{sc} (mA/cm^2)	V_{oc} (V)	FF (%)	η(%)
Safflower	1.00	0.390	24	0.100
Senna	0.37	0.371	30	0.039
Roselle	0.08	0.259	23	0.004
Rheum	0.31	0.259	27	0.022
Calumus draca	0.31	0.348	28	0.030
Carya illinoensis	0.46	0.229	18	0.025
Runica granatum	0.23	0.300	21	0.01
Rosa damascena	0.28	0.170	20	0.009

Table 2 – Parameters of the DSSCs sensitized at different temperatures, at 100 mW/cm^2 illumination

Temperature(°C)	250	300	350	400	450	500	600
J_{sc} (mA/cm^2)	0.24	0.12	0.17	1.00	0.71	0.44	0.07
V_{oc}(V)	0.229	0.229	0.230	0.390	0.377	0.374	0.259

Table 3 – Photovoltaic parameters of the DSSCs sensitized by safflower dye, at different ZnO thicknesses and 100 mW/cm^2 illumination

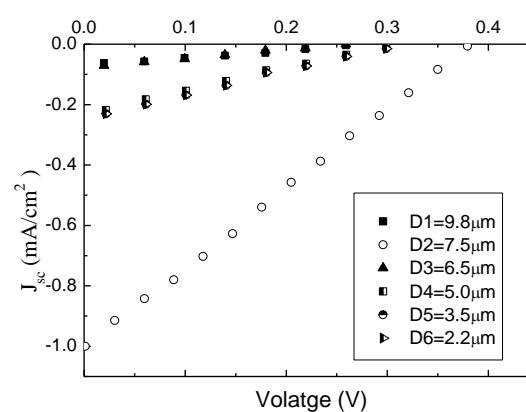| Thickness (μm)	9.8 ± 0.5	7.5 ± 0.5	6.5 ± 0.5	5 ± 0.5	3.5 ± 0.5	2.2 ± 0.5
J_{sc} (mA/cm^2)	0.075	1.00	0.33	0.07	0.22	0.23
V_{oc} (V)	0.266	0.390	0.269	0.262	0.303	0.303
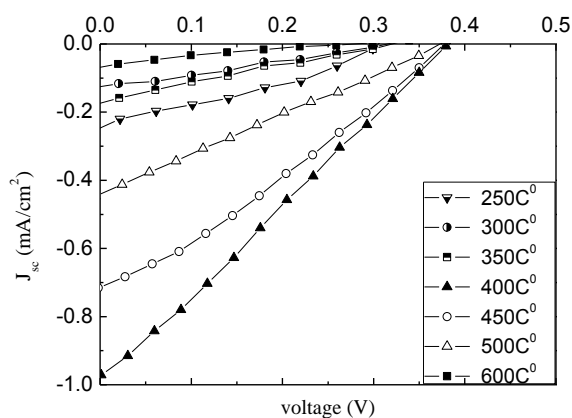
Fig. 8 – Current density-voltage characteristics of the DSSCs dyed with safflower at various photoelectrode sintering temperatures

Fig. 9 – Current density-voltage characteristics of the DSSCs prepared at different thicknesses and sensitized by safflower at 100 mW/cm^2 illumination

B. Effect of Photoelectrode Thickness

ZnO nanoparticle paste was prepared by dispersing ZnO nanoparticles in polyethylene glycol at different concentration ratios. The amount of polyethylene glycol was fixed while the solid content of ZnO was varied to get different concentrations which yield different photelectrode thicknesses. Here, we use a sintering temperature of 400 °C which exhibits the highest photoelectrical response. The thickness of ZnO layer was measured using a general microscope based on the depth of focus [26]. The results of this investigation are given in Fig. 9 and Table 3. It is clear that the DSSC with 7.5 μm thick photoelectrode shows the highest photoelectrical response at 100 mW/cm^2 illumination.

4. CONCLUSIONS

The use of natural products as semiconductor sensitizers enables simpler and faster production of cheaper and environmentally friendly solar cells. In this work,

dye-sensitized solar cells (DSSCs) were assembled using extracts from eight natural dyes as sensitizers for nanocrystalline ZnO photoelectrodes. The ZnO nanoparticles, with crystallite mean value of 12 nm as indicated from XRD data, were synthesized at pH 12. SEM pictures and TEM micrographs of the ZnO powder revealed homogeneous and well defined nanoparticles with size of about 15 nm, and shows that the powder has a porous agglomerate structure consisting mainly of spherical crystalline particles with about 15-20 nm diameter, respectively.

Photovoltaic parameters such as short circuit current I_{sc}, open circuit voltage V_{oc}, fill factor FF, and overall conversion efficiency η for the fabricated DSSCs were determined under 100 mW/cm^2 illumination. It was found that the DSSC with safflower extract as a sensitizer showed the best performance among the other extracts. The optimal semiconductor electrode sintering temperature was found to be 400 °C whereas the highest cell response is obtained at an electrode thickness of 7.5 μm.

REFERENCES

1. B. O'Regan, M. Grätzel, *Nature* **353** No 6346, 737 (1991).
2. J. Zhao, A. Wang, M.A. Green, *Prog. Photovoltaics* **7** No 6, 471 (1999).
3. M.I. Hoffert, K. Caldeira, A.K. Jain, *Nature* **395** No 6705, 881 (1998).
4. M. Grätzel, *J. Photochem. Photobiology C: Photochem. Rev.* **4** No 2, 145 (2003).
5. K. Tennakone, G.R.R.R.A. Kumara, A.R. Kumarasinghe, P.M. Sirimanne, K.G.U. Wijayantha, *J. Photochem. Photobiology A: Chem.* **94** No 2, 217 (1996)
6. S. Hao, J. Wu, Y. Huang, J. Lin, *Sol. Energ.* **80** No 6, 209 (2006).
7. Y. Amao, T. Komori, *Biosens. Bioelectron.* **19** No 8, 843 (2004).
8. A.S. Polo, N.Y.M. Iha, *Sol. Energ. Mater. Sol. C.* **90** No 13, 1936 (2006).
9. C.G. Garcia, A.S. Polo, N.Y. Iha, *J. Photochem. Photobiology A: Chem.* **160** No 1-2, 87 (2003).
10. G.P. Smestad, *Sol. Energ. Mater. Sol. C.* **55** No 1-2, 157 (1998).
11. G.R. Kumara, S. Kanebo, M. Okuya, B. Onwona-Agyeman, A. Konno, K. Tennakone, *Sol. Energ. Mater. Sol. C.* **90** No 15, 1220 (2006).
12. N.J. Cherepy, G.P. Smestad, M. Grätzel, J.Z. Zang, *J. Phys. Chem. B* **101** No 45, 9342 (1997).
13. A.Y. Batniji, R. Morjan, M.S. Abdel-Latif, T.M. El-Agez, S.A. Taya, H.S. El-Ghamri, *Turk. J. Phys.* **38** No 1, 86 (2014).
14. T.M. El-Agez, S.A. Taya, K.S. ElRefi, M.S. Abdel-Latif, *Opt. Appl.* **44** No 2, 345 (2014).
15. S.A. Taya, T.M. El-Agez, M.S. Abdel-Latif, H.S. El-Ghamri, A.Y. Batniji, I.R. El-Sheikh, *Int. J. Renewable Energ. Res.* **4** No 2, 384 (2014).
16. S.A. Taya, T.M. El-Agez, K.S. ElRefi, M.S. Abdel-Latif, *Turk. J. Phys.* **39** No 1, 24 (2015).
17. H.S. El-Ghamri, T.M. El-Agez, S.A. Taya, M.S. Abdel-Latif, A.Y. Batniji, *Mater. Sci.-Poland* **32** No 4, 547 (2015).
18. K. Wongcharee, V. Meeyoo, S. Chavadej, *Sol. Energ. Mater. Sol. C.* **91** No 7, 566 (2007).
19. A.R. Hernández-Martínez, M. Estevez, S. Vargas, F. Quintanilla, R. Rodríguez, *J. Appl. Res. Technol.* **10** No 1, 38 (2012).
20. S. Rani, P. Suri, P.K. Shishodia, R.M. Mehra, *Sol. Energ. Mater. Sol. C.* **92** No 2, 1639 (2008).
21. M.S. Abdel-Latif, M.B. Abuiriban, T.M. El-Agez, S.A. Taya, *Int. J. Renewable Energ. Res.* **5** No 1, 294 (2015).
22. A. Al-Kahlout, *Thin Solid Films* **520** No 6, 1814 (2012).
23. R. Agha Baba Zadeh, B. Mazinani, A. Mirhabibi, M. Tamizifar, *J. Phys.: Conf. Ser.* **26** No 12, 312 (2011).
24. J.S. Kwon, J.T. Snook, G.M. Wardlaw, *Am. J. Clin. Nutr.* **54** No 2, 351 (1991).
25. C.M. John, *J. Am. Coll. Cardiol.* **49** No 17, 1825 (2007).
26. J. Liu, C. Tian, Z. Wang, J. Lin, *Eurasian J. Analytical Chem.* **2** No 1, 12 (2007).